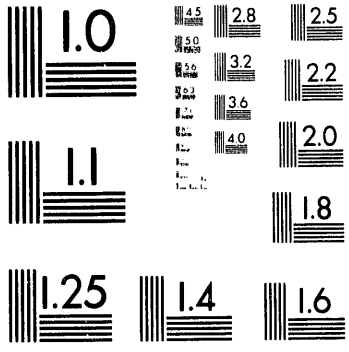
1.0
2.8
2.5
3.2
2.2
3.6
4.0
2.0
1.1
1.8
1.25
1.4
1.6

1 of 1

Role of Neutral-Beam Fueling Profile in Energy Confinement and Neutron Emission on TFTR

H.K. Park, M.G. Bell, W.M. Tang, G. Taylor, M. Yamada,
R.V. Budny, D.C. McCune, R. Wieland
Princeton Plasma Physics Laboratory
Princeton University
P. O. Box 451 Princeton, NJ 08543

Abstract

The role of the neutral-beam fueling profile in determining the stored energy and neutron emission in neutral-beam heated discharges on TFTR is investigated. It is found that the neutral-beam fueling profile is sensitive to both the magnitude and shape of the electron density. Among the plasma species, the ion stored energy is strongly correlated with the peaking of the neutral-beam fueling profile, whereas the electron stored energy is insensitive to this parameter. The D-D fusion neutron emission is also strongly correlated with the peaking of the neutral-beam fueling profile.

MASTER

1. Introduction

In intense ($P_B \gg P_{OH}$) neutral-beam-heated plasmas in the Tokamak Fusion Test Reactor (TFTR), the global energy confinement time (τ_E) ranges from $\simeq$ 50 ms to $\simeq$ 200 ms. The discharges with low τ_E are often referred to as L-mode and fit to the empirical L-mode scaling.[1] Although the characteristics of τ_E in the L-mode regime are well described by the empirical L-mode scaling relationship,[1,2] the basic physics underlying these scalings is largely unknown. Discharges with an improved energy confinement with respect to the L-mode confinement (TFTR "supershot"[3] discharges) do not follow the L-mode scaling and their τ_E is only weakly dependent on plasma current and heating power. A distinctive peaked electron density profile shape [4] and high ion temperature are major characteristics of supershot discharges.[5,6]

With respect to other measurable plasma parameters that can be correlated with the improved energy confinement and neutron emission, this paper in particular examines the role of the neutral-beam fueling profile on the stored energy and D-D fusion neutron emission. In section II, the neutral-beam fueling profile is studied as a function of target electron density profile shape and magnitude. In section III, a general description of the data set to be studied is given. The constraints on the data set and their statististical implications are also discussed. In section IV, the role of the neutral-beam fueling profile in determining the stored energy of each plasma species (ions and electrons) and the D-D fusion neutron emission is investigated.

2. Neutral-beam Fueling Deposition

Following the recent study of the neutral-beam particle deposition in TFTR, [7] the calculated neutral-beam particle deposition profile shape factor (H_{ne}) is defined as

$$H_{ne} = \frac{S_{be}(0,t)}{\langle S_{be}(r,t)\rangle}, \tag{1}$$

where $S_{be}(0,t)$ and $\langle S_{be}(r,t)\rangle$ are the central and volume-averaged electron source rates due to the neutral-beam, respectively. This definition is similar to the density peakedness factor $F_{ne} = n_e(0)/\langle n_e\rangle$, where $n_e(0)$ is the central electron density and $\langle n_e\rangle$ is volume-averaged electron density. In reference [7], it was shown that the calculation of the neutral-beam deposition in a tokamak plasma should employ both the new tabulation of atomic cross-sections[8] and Multi-Step Ionization (MSI) processes.[9] The attenuation of the injected neutral-beam is to first order proportional to the local electron density, so a peaked neutral-beam deposition profile can only be achieved at high density with a peaked density profile. In order to parameterize the expression for H_{ne} for a variety of F_{ne}, a regression has been performed for values of H_{ne} calculated by the TRANSP code[10] as a function of $\bar{n}_e$ and F_{ne}. The range of F_{ne} of this data set is from 0.5 to 5.0 (see reference [7]). Among the functional combinations, the best description is as follow:

$$H_{ne} \simeq \alpha\, F_{ne}^{\beta}\, exp\,[-\gamma\, \bar{n}_e], \tag{2}$$

where α, β and γ are regression coefficients appropriate to the TFTR data base. The calculated H_{ne} using old atomic cross-sections (σ_1), or σ_1 and MSI processes and new atomic cross-sections (σ_2) has been fitted to Eq. 2. The regression coefficients are shown in Table 1.

cross - section	*symbol*	α	β	γ
σ_1	○	2.41	1.04	0.24×10^{-19}
$\sigma_1 + MSI$	△	2.86	1.07	0.33×10^{-19}
σ_2	□	2.49	0.90	0.18×10^{-19}

Table 1: Coefficients for H_{ne} are evaluated using various cross-sections: σ_1 uses the old tabulation of atomic cross-sections, σ_2 uses the new tabulation of atomic cross-sections, and σ_1 + MSI uses the old cross-section plus MSI model

The ratio of the calculated H_{ne} to the fitted H_{ne} is illustrated as a function of $\bar{n}_e$ in Fig. 1. The relationship in Eq.(2) shows that a peaked electron density profile

shape is essential for peaked deposition of the neutral-beam at high density. Since the calculation with both σ_2 and MSI processes is not available, the coefficients evaluated using only σ_1 will be used in the regression study (see reference [7]).

Note that H_{ne} is different from the conventional neutral-beam power deposition peaking factor ($H(0)$, where $H(0)$ is defined as the ratio of the central neutral-beam power per unit volume to the volume averaged power) due to the presence of fractional energy components ($E/2$, and $E/3$) in the heating-beam. If the beam has only a full energy component, H_{ne} is the same as $H(0)$. In addition to the magnitude and profile shape of the electron density, there are many other machine parameters which can influence H_{ne} such as beam energy, angle of injection, beam size, plasma size (major and minor radius) and plasma cross-sectional shape (circular or non-circular). Therefore, this parameter should be determined considering these engineering and physical parameters for each experiment. For example, at the same line average density, a non-circular plasma ($\kappa \geq 1$) will have higher H_{ne} than a circular plasma due to the volume effect.

Using the measured $F_{ne}(t)$ and $\bar{n}_e(t)$, it is instructive to examine the time dependence of H_{ne} together with other plasma parameters for typical TFTR discharges. Fig. 2 shows the temporal evolution of H_{ne} for L-mode and supershot discharges for the same beam power ($P_B \simeq 22\ MW$). In the supershot, the initial central beam fueling is significantly better compared to the L-mode due to differences in the pre-beam electron density. The initial high level of central beam fueling is maintained ($H_{ne} \simeq 3.0$) as $\bar{n}_e$ is increased, until a "Carbon bloom"[11] (accompanied by a sudden rise of edge electron density) occurs at about 3.8 sec. The degradation of W_{tot} and neutron emission (S_n) is well correlated with the reduction in H_{ne} ($\simeq 3.0$ to $\simeq 1.0$). For the L-mode plasma, the low initial beam fueling ($H_{ne} \simeq 1.0$) falls rapidly to $\simeq 0.3$ so that after that time of NBI, there is almost an order of magnitude difference in H_{ne} between the supershot and L-mode plasmas. It is striking, however, that the accumulated W_e in each discharge is similar in magnitude. This result implies that W_i

in the supershot discharge is significantly greater than that of the L-mode discharge. The D-D fusion neutron emission in the L-mode discharge is an order of magnitude smaller than that of the supershot discharge.

3. Data base and Constraints

This study involves approximately 870 TFTR deuterium discharges, constrained to deuterium gas fueled discharges only. The data points consist of each plasma parameter at the peak time of the global stored energy. Wide range of beam power ($5 \leq P_B \leq 32\ MW$) and plasma current ($0.9\ MA \leq I_P \leq 2.0\ MA$) are included. Here, discharges with plasma current ramps during the heating pulse are excluded. In all discharges, the beam power exceeds the Ohmic power by a factor of ≥ 5 to reduce the influence of Ohmic heating on the confinement. Deuterium beams with 90 keV $\leq E_{inj} \leq$ 110 keV are injected tangentially and data are restricted to nearly balanced injection, *i.e.*, $|(P_{co} - P_{ctr})/(P_{co} + P_{ctr})| \leq 0.4$, where the subscript *co* and *ctr* refer to injection in the same and opposite direction with respect to the plasma current, respectively. The neutral particle ratio used in this paper is $D^0[E]$:$D^0[E/2]$:$D^0[E/3]$ = 0.44:0.30:0.26. The total stored energy (W_{tot}) is determined from magnetic measurements,[12] so that both the thermal and fast-beam ion energies are included. The electron stored energy (W_e) is calculated[4] using the inverted electron density profile[13] measured by multi-channel interferometry[14] and the electron temperature profile measured by ECE radiometry.[15] The ion stored energy (W_i) is simply $W_{tot} - W_e$.

In a statistical study, it is important to isolate the inter-correlation between the assumed independent parameters. In order to eliminate other possible strong parametric dependences, this data set is constrained to fixed plasma major and minor radii of R = 2.45 m, and a = 0.8 m. The toroidal magnetic field is B_T = 4.0 T and 4.8 T. B_T and E_{inj} can be used as independent parameters but their variation is too small to show explicit dependences. There are many other plasma parameters that can be

correlated with the performance of discharges such as the pre-beam electron density and carbon intensity which can be a measure of the wall recycling condition. It is expected that H_{ne} is well correlated with the condition of the wall recycling. H_{ne} will be added as an independent parameter in addion to I_P, and P_B. These parameters are not completely independent due to the operational constraints in experiments. However, with the inclusion of L-mode data, the inter-correlations between these parameters are minimized. For instance, the upper limit of P_B can be raised as I_P is increased due to the β-limit as shown in Fig. 3a. Similarly, the achieved upper limit of H_{ne} is reduced as I_P is increased as shown in Fig. 3b. The upper limit of H_{ne} is slightly reduced as P_B is increased as shown in Fig. 3c.

As shown in the previous section for a fixed plasma geometry, H_{ne} is sensitive only to the electron density and its profile shape. Therefore the reduced upper limit of H_{ne} at higher I_P must be interpreted as the higher electron density and/or broader profile shape. It is important to know whether the increased electron density at higher applied plasma current is due to the improved particle confinement time or increased wall recycling for a carbon limiter. Since similar wall conditioning techniques have been applied for the carbon limiter, it seems likely that the improved intrinsic particle confinement time at higher I_P may be responsible for the increased electron density. Note that the pre-beam and edge electron density can be lowered at higher plasma current using lithium pellets in TFTR.[16]

4. Role of H_{ne} on Stored Energy and Neutron Emission

Although several regimes of enhanced energy confinement relative to the L-mode predictions have been produced in TFTR,[5,6] we will concentrate in this section on the role of H_{ne} in the variation of energy confinement and D-D fusion neutron emission from L-mode to supershots.

Among other distinctive characteristics, the performance of the beam-heated dis-

charge has been strongly correlated with the peakedness of the electron density profile[4]. Although There has been an attempt to interpret the observed correlation with the transport physics associated with the density gradient, the results were not conclusive[17]. This is due in large part to the fact that the physics of the time evolution of these discharges is extremely complicated as a result of the rapid simultaneous changes of many plasma parameters and their profiles. It is important to note that a peaked electron density profile alone is not a sufficient condition to improve stored plasma energy in beam heated discharges in TFTR. When high density ohmically heated target plasmas, fueled with solid deuterium pellets were heated with beams, the resulting stored energy was generally similar to L-mode discharges, even though the electron density profiles were highly peaked. This observation leads to the conclusion that the peakedness of the electron density profile is not sufficient to improve the confinement and that the observed peaked electron density profile in the supershot discharge may be due to different causes. When H_{ne} was evaluated for the discharges, the value was found to be very low (in general $H_{ne} \leq 1.5$). When H_{ne} was high (≥ 3.0) for these discharges, the stored energy and neutron emission were significantly improved over that of L-mode discharges. We are led to the hypothesis that the observed correlation between the improved energy confinement and peaking of the density profile may originate from the fact that central penetration of the beam can only be achieved with a peaked density profile at high density and the peaked electron density profile will result from the peaked beam deposition.

Considering the observed high central ion temperature and low central impurity level in a good supershot plasma, the improved global energy confinement is largely due to the ions rather than electrons as shown in Fig. 4. Here, the fraction of stored energy of the ions is depicted as a function of central beam fueling parameter, $P_B H_{ne}$. Up to $P_B H_{ne} \simeq 25\ MW$, the ion fraction increases rapidly and the ratio saturates at about $\simeq 0.7$. Note that W_i consists of both thermal and fast beam-ions. In principle, the stored energy of fast-beam ions should be studied separately from thermal ions

to determine if there are differences in their confinement properties. Since, there are practical problems such as precise information regarding local ion density and slowing down time at high ion temperature, the ion stored energy will not be treated separately in this paper.

The variation of ion stored energy is illustrated as a function of P_B in Fig. 5a. It will be shown that the observed variation can be significantly reduced by additional parameters (H_{ne}, and I_P). Most importantly, the role of H_{ne} is more significant than that of I_P. The regression result of the ion stored energy shows that the the goodness of fit (R^2) is 0.95 and is given in the below;

$$W_i(MJ) \simeq C\ P_B^{1.21\pm0.01}(MW)\ H_{ne}^{0.90\pm0.01}\ I_P^{0.38\pm0.02}(MA), \tag{3}$$

where C is 2.14 $\times 10^{-2}$. Note that the plasma parameters used in this study are at the peak time of W_{tot}. When the regression was performed without I_P, the R^2 value was 0.93 with slightly different coefficients ($W_i \propto P_B^{1.30} H_{ne}^{0.81}$). This result indicates that the role of H_{ne} is significantly more important than that of I_P in determining the ion stored energy. In order to demonstrate the significance of H_{ne}, a similar regression is performed for W_i with P_B and H_{ne} as independent parameters at a fixed I_P group. The regression coefficients and goodness of fit (R^2) for $W_i \propto P_B^{\alpha\pm\Delta\alpha}\ H_{ne}^{\beta\pm\Delta\beta}$ are summarized in Table 2. The results demonstrated in Fig. 5b and Table 2, lead

Plasma Current	*Data Points*	R^2	α	$\Delta\alpha$	β	$\Delta\beta$
$I_P = 0.9/1.0MA$	276	0.93	1.19	±0.04	1.04	±0.02
$I_P = 1.4/1.6MA$	364	0.95	1.26	±0.02	0.88	±0.01
$I_P = 1.8/2.0MA$	228	0.97	1.19	±0.01	0.79	±0.02

Table 2: Coefficients of the regression results are evaluated for each plasma current group. The role of H_{ne} on the ion stored energy is not altered by an absence of I_P. $W_i \propto P_B^{\alpha\pm\Delta\alpha}\ H_{ne}^{\beta\pm\Delta\beta}$ is used for each I_P group.

to the conclusion that the central beam fueling ($P_B H_{ne}$) is strongly correlated the observed ion stored energy for any plasma current.

On the other hand, the electron stored energy is not as well correlated ($R^2 = 0.80$) with the same set of independent parameters and the result is given as;

$$W_e(MJ) \simeq C\ P_B^{0.68\pm0.02}\ I_P^{0.47\pm0.03}\ H_{ne}^{0.12\pm0.01}, \tag{4}$$

where C is 7.6×10^{-2}. It is surprising that the parameteric dependence of electron stored energy is significantly different from that of ions. When the regression was performed without H_{ne}, R^2 was reduced from 0.8 to 0.77 and $W_e \propto P_B^{0.68}\ I_P^{0.37}$. Certainly H_{ne} was important in determination of ion energy but not important at all in electron stored energy.

Due to the dominance of the ion stored energy in supershots, any global scalings for the energy confinement simply represent the trend of ion confinement and have little to do with the nature of electron confinement. If H_{ne} is assumed to be propotional to the power deposition peaking factor ($H(0)$), the exisisting theoretical model for the influence of $H(0)$ on the global stored energy[18], which is based on a single fluid model may not be suitable for beam-heated plasmas.

In fusion plasma studies, the ultimate goal is the production of fusion power which is proportional to the neutron emission rate (S_n). In TFTR, S_n from D-D reactions has been strongly correlated with the square of the total stored energy ($\propto W_{tot}^2$)[5] and the upper bound of S_n has been scaled with the beam power ($\propto P_B^{1.8}$)[20,21]. Based on the results in Eqs. 3 and 4, the two scalings must be closely related through the ion stored energy. Using the same set of independent parameters employed in the study of energy confinement, a regression is performed for S_n and the result is given as follow;

$$S_n\ (/sec.) \simeq C\ P_B^{2.09\pm0.02}(MW)\ H_{ne}^{1.40\pm0.02}\ I_P^{0.31\pm0.04}(MA), \tag{5}$$

where C is 1.00×10^{13} and R^2 is 0.96. The fitted data to this result is shown in Fig. 6 and the neutron emission is dominated by P_B and H_{ne}. When the same regression was performed without including the plasma current, R^2 was reduce from 0.96 to 0.95 with slightly different coefficients ($S_n \propto P_B^{2.19}\ H_{ne}^{1.34}$). Similar to the ion stored

energy case, the significance of H_{ne} is examined for each of the plasma current groups and the results are summarized in Table 3.

Plasma Current	*Data Points*	R^2	α	$\Delta\alpha$	β	$\Delta\beta$
$I_P = 0.9/1.0MA$	338	0.91	2.02	± 0.05	1.29	± 0.03
$I_P = 1.4/1.6MA$	338	0.97	2.29	± 0.04	1.46	± 0.02
$I_P = 1.8/2.0MA$	202	0.97	2.02	± 0.03	1.34	± 0.04

Table 3: Coefficients of the regression results are evaluated for each plasma current group. The role of H_{ne} on the neutron emission is not altered by an absence of I_P. $S_n \propto P_B^{\alpha \pm \Delta\alpha}\ H_{ne}^{\beta \pm \Delta\beta}$ is used for each I_P group.

Although the role of H_{ne} is significant in determining the stored energy of ions and neutron emission, there are variations among the discharges with similar value of H_{ne}. Since the direct measurement of H_{ne} is not available, the variation may be due to many other factors such as errors in H_{ne} estimation, differences in time history of H_{ne}, the effect of MHD on ions (thermal and fast ions)[19], and/or other unknown transport mechanisms.

5. Summary

In summary, the neutral-beam fueling peaking factor (H_{ne}) is determined by both the magnitude of the target electron density and its profile shape for the fixed engineering parameters of the heating-beam system and tokamak, such as beam size, beam energy, orientation, and plasma sizes. In this paper, it has been shown that the role of H_{ne} is significant in determining the ion stored energy and D-D fusion neutron rate in beam-heated plasmas in TFTR. However, the electron strored energy is found to be insensitive to H_{ne}. The present study suggests that any realistic scalings based on geometric factors in beam-heated plasmas should take into acount the variations in H_{ne}. In addition, a better theoretical model for the influence of H_{ne} (or $H(0)$) on

confinement as a function of plasma species is needed in order to extend the results of the present investigations to other heating schemes.

6. Acknowlegement

The authors wish to thank the TFTR staff who contributed to the completion of this work. One of the authors (H. Park) deeply appreciates special encouragement from Drs. N. Bretz, L.C. Johnson, J.S. Machuzak, K.M. McGuire, D. Meade, J.D. Strachan, and K.M. Young to finish this paper. He also wishes to thank Drs. Z. Chang, J. Callen, and D. Mikkelson for illuminating discussions. This work was supported by U.S. DoE contract No. DE-ACO2-76-CHO-3073.

References

[1] Goldston R.J., Plasma Phys. **26**, 87 (1984).

[2] Rebut, P.H., Lallia, P.P., Watkins, M.L., in Plasma Physics and Controlled Nuclear Fusion Research 1988 (Pro. 12th Int. Conf. Nice, 1988), Vol.2, IAEA, Vienna (1989) 191.

[3] Strachan, J.D., Bell, M.G., *et al.*, Phys. Rev. Lett. **58** (1987) 1004.

[4] Park, H.K., Goldston, R.J., and Taylor, G., in Proceedings of the 4th international Symposium on Laser-Aided Plasma Diagnostics, (Fukuoka , Japan, Nov. 1989)

[5] Bell, M.G., Arunasalum, V., Barnes, C., *et al.* in Plasma Physics and Controlled Nuclear Fusion Research 1988 (Pro. 12th Int. Conf. Nice, 1988), Vol.1, IAEA, Vienna (1989) 27.

[6] Meade, D., Arunasalum, V., Barnes, C., *et al.* in Plasma Physics and Controlled Nuclear Fusion Research 1990 (Pro. 13th Int. Conf. Washington D.C., 1990) Vol.1, IAEA, Washington D.C., (1991) 9-26.

[7] Park, H.K., Barnes, C.W., Budny, R., *et al.*, Nucl. Fusion **32** (1992) 1042.

[8] Barnett, C.F., Atomic data for fusion, ORNL-6086, Vol-1, Controlled Fusion Atomic Data Center, ORNL, (July, 1990)

[9] Janev, R.K., Boley, C.D., Post, D.E., Nucl. Fusion **29** (1989) 2125.

[10] Hawryluk, R.J., in Physics of Plasma Close to Thermonuclear Conditions (Proc. Cource Varenna, 1979), Vol. 1, CEC, Brussels (1980) 19.

[11] Ramsey, A., C. E. Bush, H. F. Dylla, *et al.*, Nucl. Fusion **31** (1991) 1811.

[12] Bell, M.G., Arunasalam, V., Bitter, M., *et al.*, Plasma Phys. Controlled Fusion **28** (1986) 1392.

[13] Park, H.K., Plasma Phys. Controlled Fusion **31**, 2035, (1989).

[14] Mansfield, D.K., Park, H.K., Johnson, L.C., *et al.*, Appl. Optics, **15**, 4469, (1987) Japan, Nov. 1989)

[15] Taylor, G., Efthimion, P.C., McCarthy, M.P., *et al.*, Rev. Sci. Insrum. **57**, 1974 (1986)

[16] Snipes, J.A., Terry, J.L., Marmar, E.S., *et al.* in proceedings of the 18th European Conference on Controlled Fusion and Plasma Heating, Berlin, 1991, Vol. 1, 42-45, EPS, 1991.

[17] Zarnstorff, M., Bateman, G., Batha, S., *et al.* Paper IAEA-CN-56/A-2-2 presented at the 14th Internation Conference on Plasma Physics and Controlled Nuclear Fusion Research (Wurzburg, Germany, 1992)

[18] Callen, J.D., Christiansen, J.P., Cordey, J.G., *et al.*, Nucl. Fusion, **27**, (1987) 1857

[19] Chang, Z., Fredrickson, E.D., Callen, J.D., *et al.* to be published in proceedings of the 20th European Conference on Controlled Fusion and P lasma Heating, Lisbon, 1993, Vol. 1, 42-45, EPS, 1993.

[20] Jassby, D.L., Arunasalum, V., Barnes, C.,*et al.* Phys. of Fluids **B3** (1991) 2308.

[21] Strachan, J.D., Bell, M.G., Bitter, M., *et al.* Princeton Plasma Physics Laboratory Report, PPPL-2858, (Oct.) 1992

Figure 1 The ratio between the calculated and fitted H_{ne} as a function of $\bar{n}_e$ for a various F_{ne} with a fixed plasma minor (a_O = 0.8 m) and major (R_O = 2.45 m) radii. H_{ne} is calculated by the three different methods: o – using old taulation of atomic cross-section (σ_1), $\triangle$ – using σ_1 with the old MSI model, and $\square$ – using new tabulation of atomic cross-section (σ_2). The evaluated coefficients are summarized in Table 1.

Figure 2 The temporal evolution of H_{ne} based on Eq. 1 with other plasma parameters such as global stored energy (W_{tot}), stored energy of electrons (W_e), and neutron emission (S_n) for the same heating-beam power ($P_B \simeq 22\ MW$); thick — - "supershot" discharge at $I_P = 1.4\ MA$ and — - L-mode discharge at $I_P = 2.0\ MA$. Average H_{ne} value of the supershot is an order of magnitude higher than that of L-mode for the first half second.

Figure 3 The level of inter-correlation between the chosen independent parameters is illustrated. (a) Heating-beam power (P_B) used in the experiment for each plasma current is illustrated. (b) The achieved H_{ne} is shown as a function of plasma current. (c) The achieved H_{ne} for an applied P_B is shown.

Figure 4 The ratio of the ion stored energy to the global stored energy as a function of $P_B H_{ne}$ is illiustrated; As $P_B H_{ne}$ is increased up to 25 MW, W_i/W_{tot} is rapidly improved. Above this value, the ratio is saturated ($W_i/W_{tot} \simeq 0.7$).

Figure 5 (a) The stored energy of ion is depicted as a function of P_B. For a fixed P_B, various value of the stored energy is obtained. (b) The stored energy of ion is fitted to the regression result shown in Eq. 3. Note that W_i is linearly proportional to the central heating-beam fueling ($P_B H_{ne}$ and I_P is not a significant factor.

Figure 6 The D-D fusion neutron emission (S_n) is fitted to the regression result shown in Eq. 5. S_n is independent of plasma current.

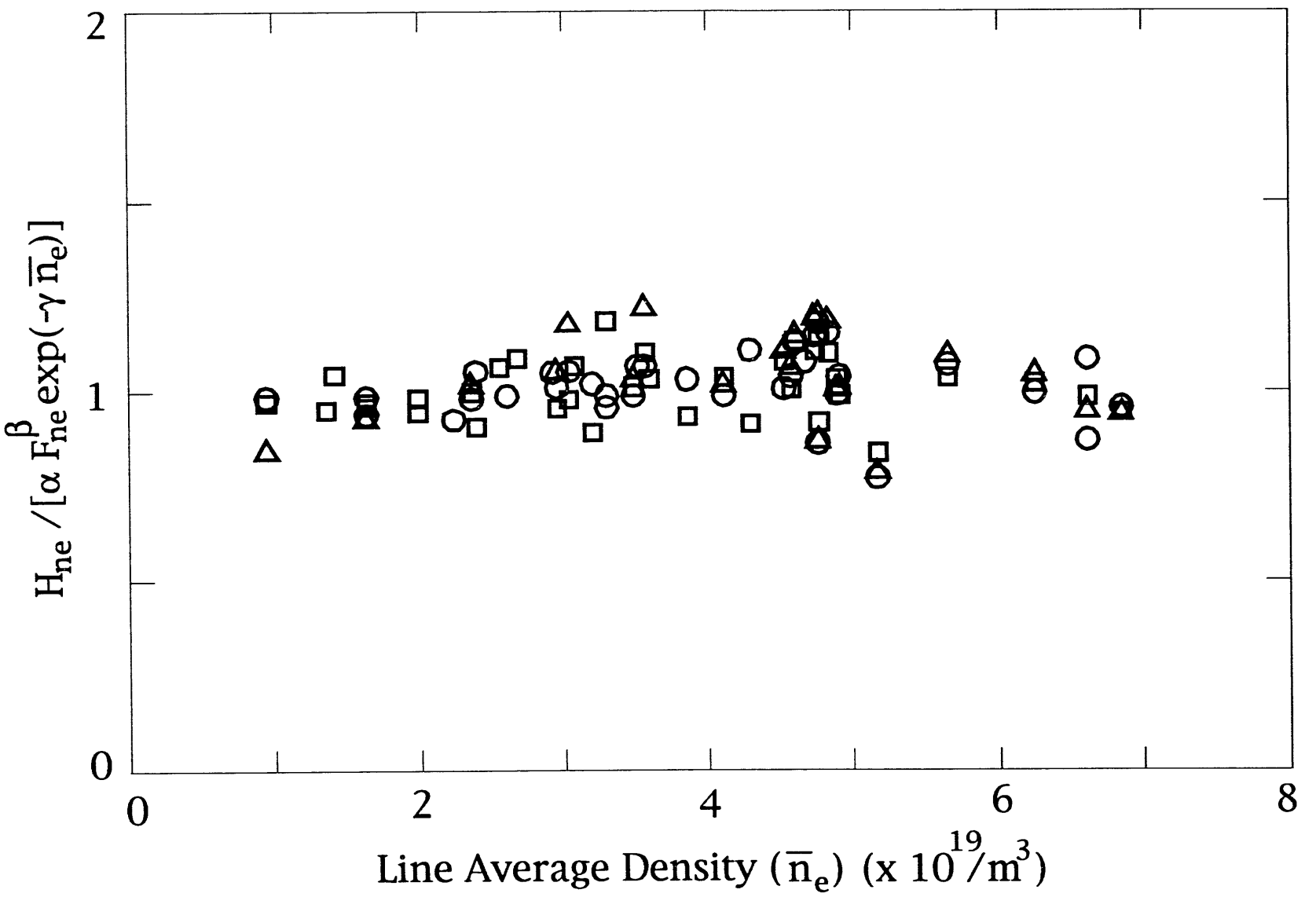
2
1
0
0
2
4
6
8
$H_{ne} / [\alpha F_{ne}^{\beta} \exp(-\gamma \bar{n}_e)]$
Line Average Density ($\bar{n}_e$) (x $10^{19}/m^3$)

Figure 1

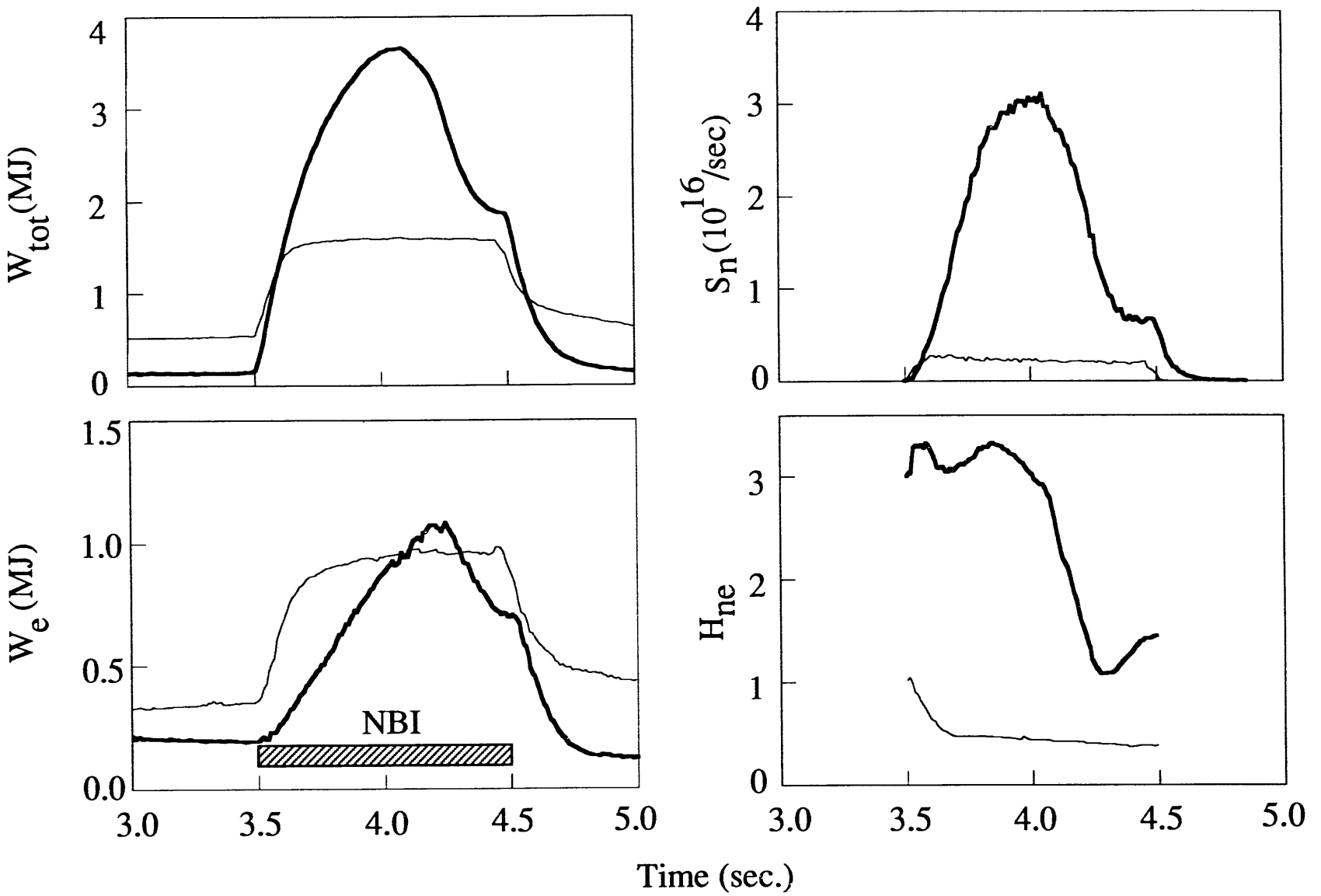
W_{tot}(MJ)
$S_n(10^{16}/sec)$
W_e (MJ)
H_{ne}
NBI
Time (sec.)
0
1
2
3
4
0.0
0.5
1.0
1.5
3.0
3.5
4.0
4.5
5.0

Figure 2

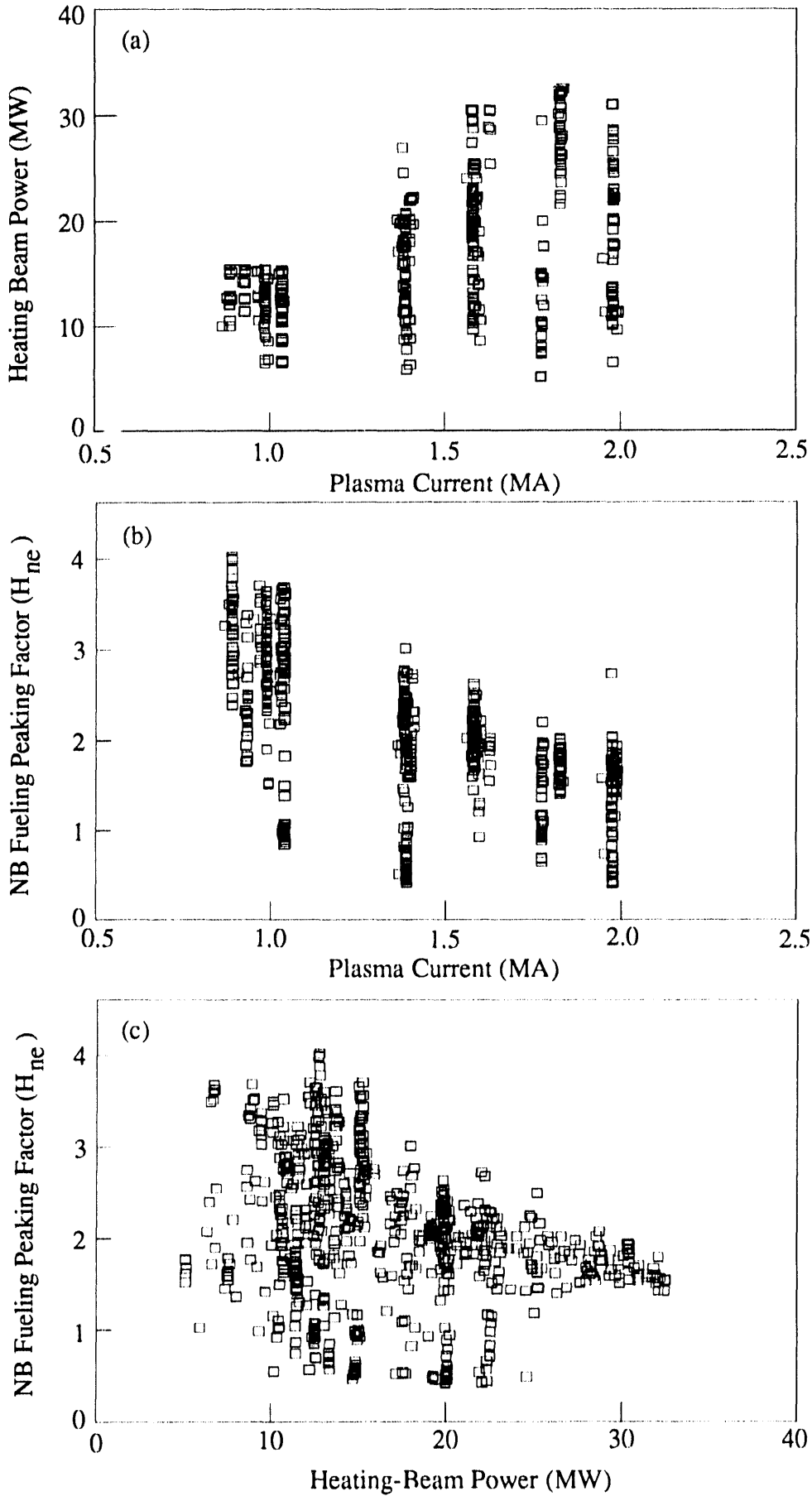
(a)
Heating Beam Power (MW)
0
10
20
30
40
0.5
1.0
1.5
2.0
2.5
Plasma Current (MA)
(b)
NB Fueling Peaking Factor (H_{ne})
0
1
2
3
4
0.5
1.0
1.5
2.0
2.5
Plasma Current (MA)
(c)
NB Fueling Peaking Factor (H_{ne})
0
1
2
3
4
0
10
20
30
40
Heating-Beam Power (MW)

Figure 3

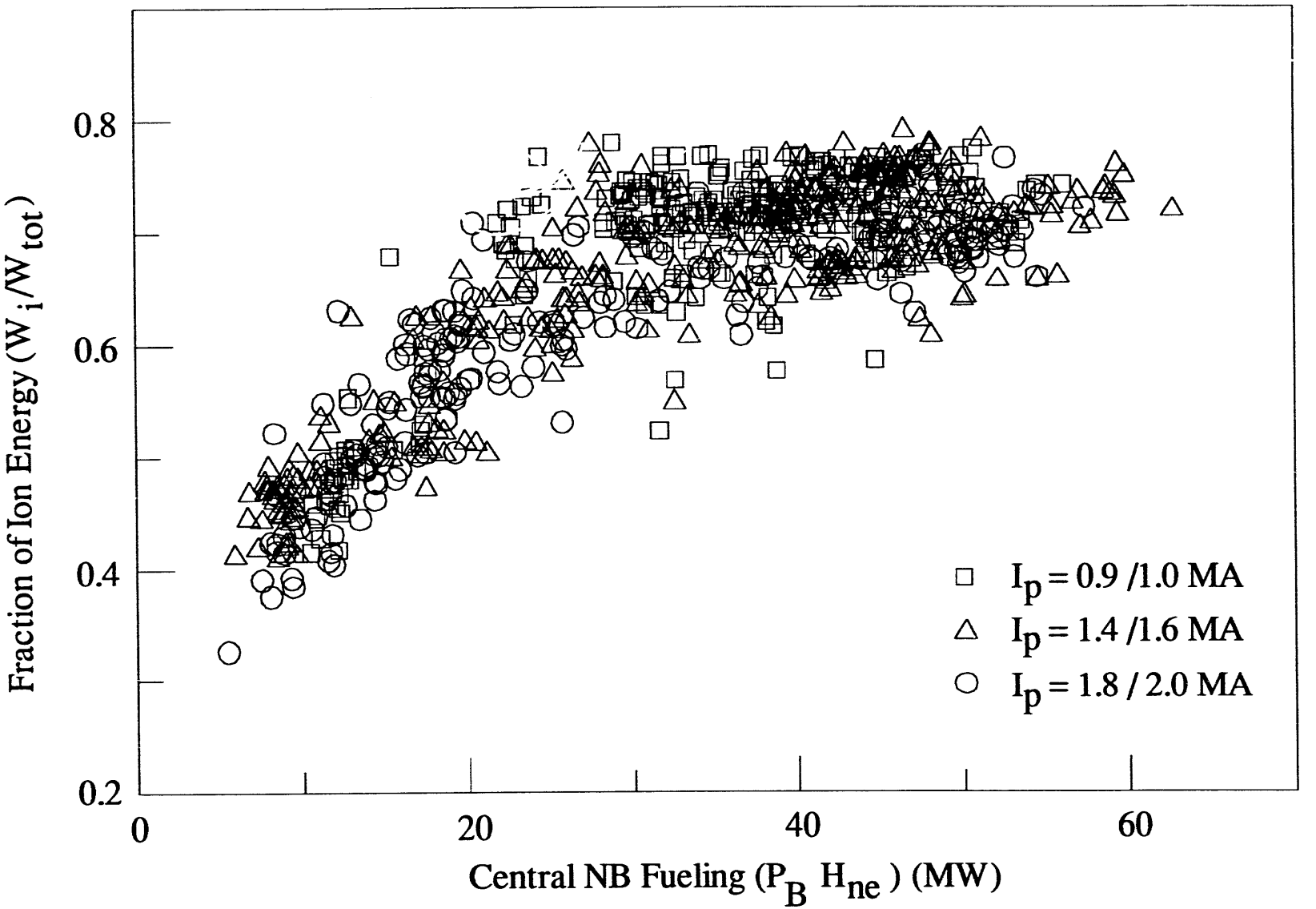
0.8
0.6
0.4
0.2
0
20
40
60
Fraction of Ion Energy (W_i/W_{tot})
Central NB Fueling (P_B H_{ne}) (MW)
I_p = 0.9 /1.0 MA
I_p = 1.4 /1.6 MA
I_p = 1.8 / 2.0 MA

Figure 4

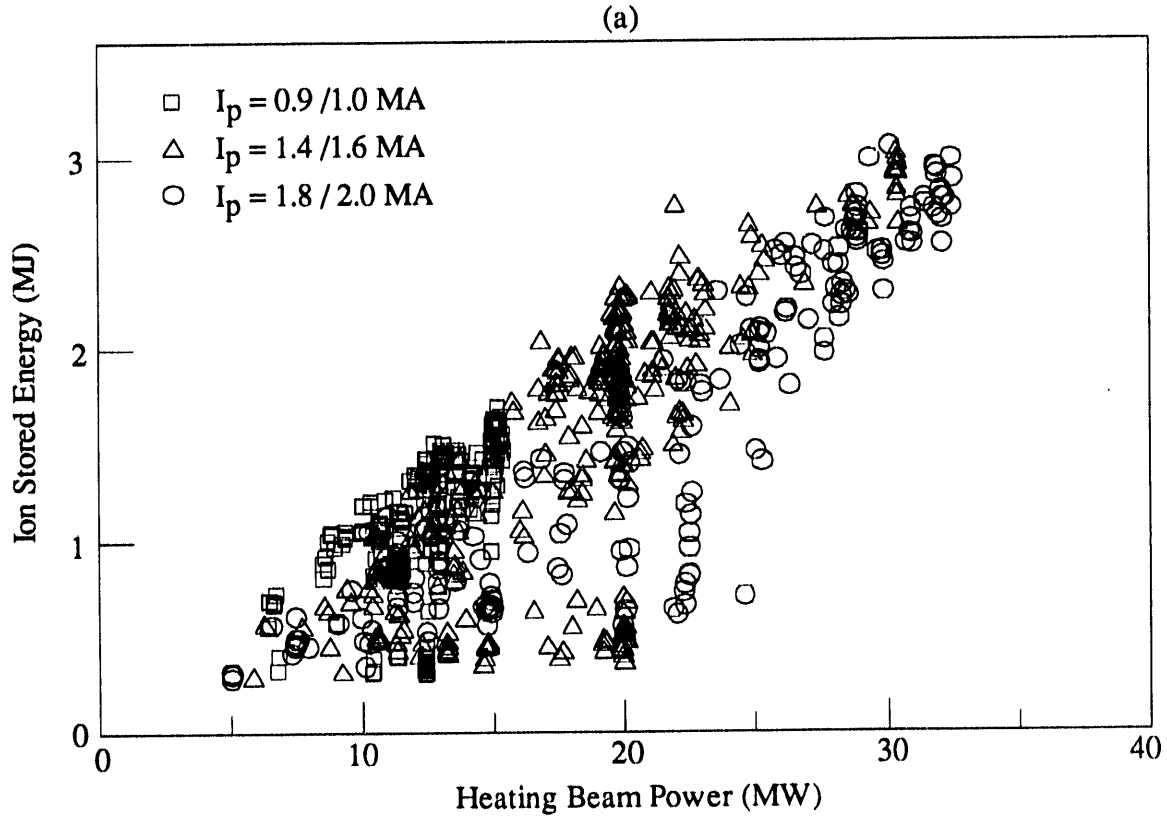

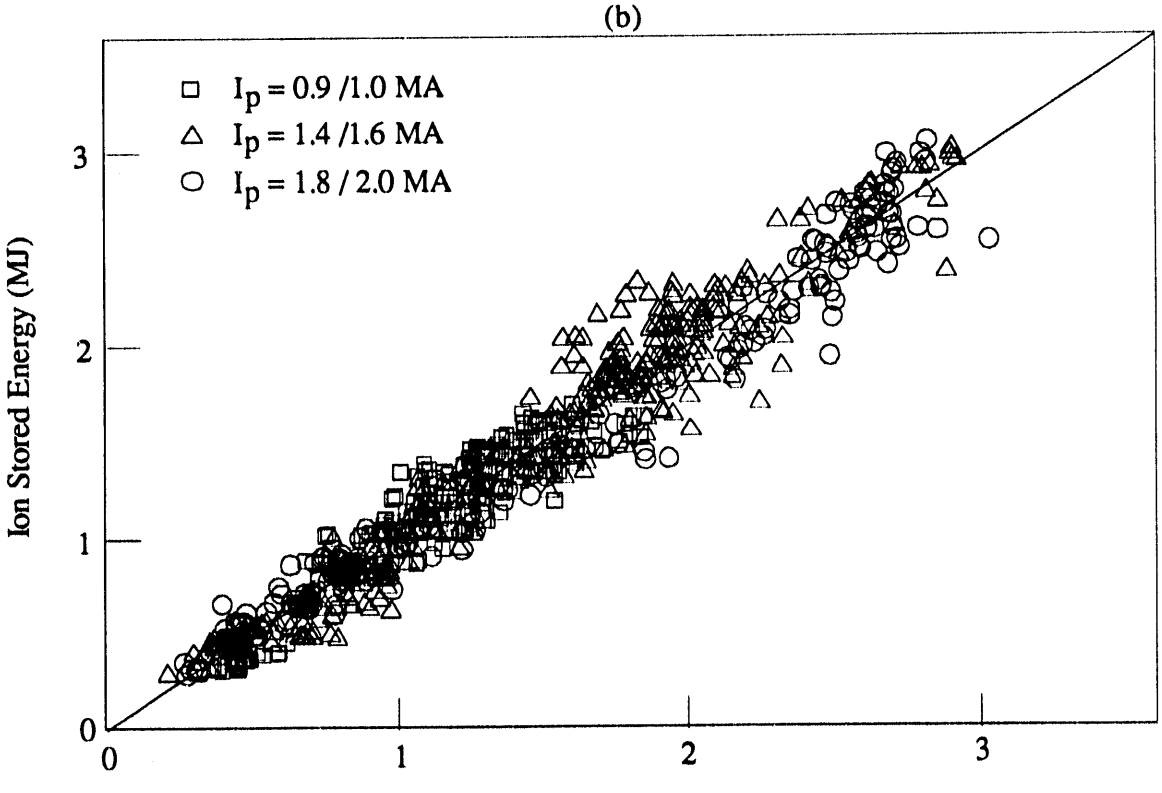

$$W_i\,(\mathrm{MJ}) \cong 2.14 \times 10^{-2} P_B^{1.21}\,(\mathrm{MW})\, H_{ne}^{0.90} I_p^{0.38}\,(\mathrm{MA})$$

Figure 5

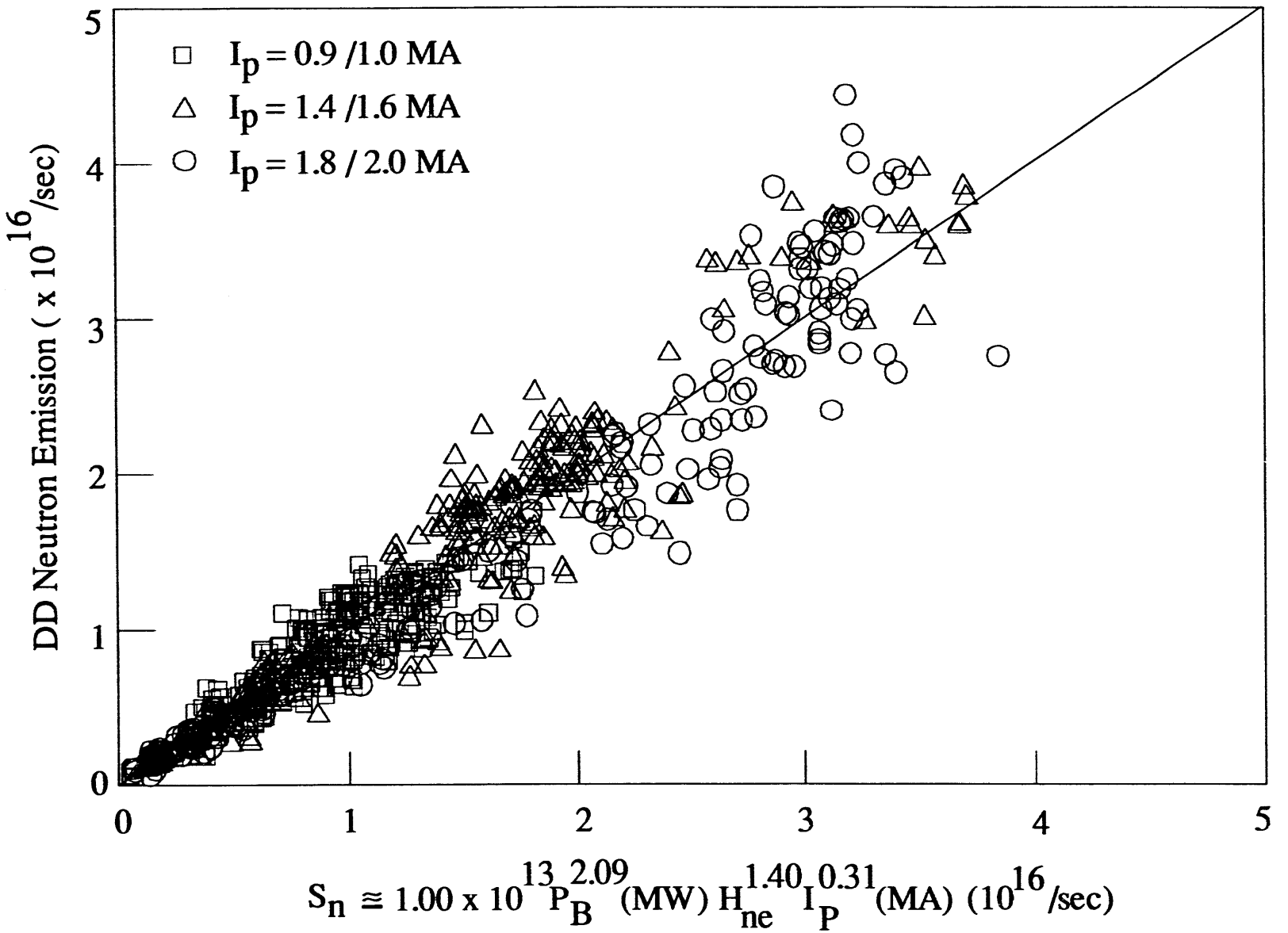
I_p = 0.9 /1.0 MA
I_p = 1.4 /1.6 MA
I_p = 1.8 / 2.0 MA
DD Neutron Emission (x 10^{16}/sec)
0
1
2
3
4
5
$S_n \cong 1.00 \times 10^{13} P_B^{2.09}$ (MW) $H_{ne}^{1.40} I_P^{0.31}$ (MA) (10^{16}/sec)

Figure 6

EXTERNAL DISTRIBUTION IN ADDITION TO UC-420

Dr. F. Paoloni, Univ. of Wollongong, AUSTRALIA
Prof. M.H. Brennan, Univ. of Sydney, AUSTRALIA
Plasma Research Lab., Australian Nat. Univ., AUSTRALIA
Prof. I.R. Jones, Flinders Univ, AUSTRALIA
Prof. F. Cap, Inst. for Theoretical Physics, AUSTRIA
Prof. M. Heindler, Institut für Theoretische Physik, AUSTRIA
Prof. M. Goossens, Astronomisch Instituut, BELGIUM
Ecole Royale Militaire, Lab. de Phy. Plasmas, BELGIUM
Commission-European, DG. XII-Fusion Prog., BELGIUM
Prof. R. Boucique, Rijksuniversiteit Gent, BELGIUM
Dr. P.H. Sakanaka, Instituto Fisica, BRAZIL
Instituto Nacional De Pesquisas Especiais-INPE, BRAZIL
Documents Office, Atomic Energy of Canada Ltd., CANADA
Dr. M.P. Bachynski, MPB Technologies, Inc., CANADA
Dr. H.M. Skarsgard, Univ. of Saskatchewan, CANADA
Prof. J. Teichmann, Univ. of Montreal, CANADA
Prof. S.R. Sreenivasan, Univ. of Calgary, CANADA
Prof. T.W. Johnston, INRS-Energie, CANADA
Dr. R. Bolton, Centre canadien de fusion magnétique, CANADA
Dr. C.R. James,, Univ. of Alberta, CANADA
Dr. P. Lukác, Komenského Universzita, CZECHO-SLOVAKIA
The Librarian, Culham Laboratory, ENGLAND
Library, R61, Rutherford Appleton Laboratory, ENGLAND
Mrs. S.A. Hutchinson, JET Library, ENGLAND
Dr. S.C. Sharma, Univ. of South Pacific, FIJI ISLANDS
P. Mähönen, Univ. of Helsinki, FINLAND
Prof. M.N. Bussac, Ecole Polytechnique,, FRANCE
C. Mouttet, Lab. de Physique des Milieux Ionisés, FRANCE
J. Radet, CEN/CADARACHE - Bat 506, FRANCE
Prof. E. Economou, Univ. of Crete, GREECE
Ms. C. Rinni, Univ. of Ioannina, GREECE
Dr. T. Mual, Academy Bibliographic Ser., HONG KONG
Preprint Library, Hungarian Academy of Sci., HUNGARY
Dr. B. DasGupta, Saha Inst. of Nuclear Physics, INDIA
Dr. P. Kaw, Inst. for Plasma Research, INDIA
Dr. P. Rosenau, Israel Inst. of Technology, ISRAEL
Librarian, International Center for Theo Physics, ITALY
Miss C. De Palo, Associazione EURATOM-ENEA , ITALY
Dr. G. Grosso, Istituto di Fisica del Plasma, ITALY
Prof. G. Rostangni, Istituto Gas Ionizzati Del Cnr, ITALY
Dr. H. Yamato, Toshiba Res & Devel Center, JAPAN
Prof. I. Kawakami, Hiroshima Univ., JAPAN
Prof. K. Nishikawa, Hiroshima Univ., JAPAN
Director, Japan Atomic Energy Research Inst., JAPAN
Prof. S. Itoh, Kyushu Univ., JAPAN
Research Info. Ctr., National Instit. for Fusion Science, JAPAN
Prof. S. Tanaka, Kyoto Univ., JAPAN
Library, Kyoto Univ., JAPAN
Prof. N. Inoue, Univ. of Tokyo, JAPAN
Secretary, Plasma Section, Electrotechnical Lab., JAPAN
S. Mori, Technical Advisor, JAERI, JAPAN
Dr. O. Mitarai, Kumamoto Inst. of Technology, JAPAN
J. Hyeon-Sook, Korea Atomic Energy Research Inst., KOREA
D.I. Choi, The Korea Adv. Inst. of Sci. & Tech., KOREA
Prof. B.S. Liley, Univ. of Waikato, NEW ZEALAND
Inst of Physics, Chinese Acad Sci PEOPLE'S REP. OF CHINA
Library, Inst. of Plasma Physics, PEOPLE'S REP. OF CHINA
Tsinghua Univ. Library, PEOPLE'S REPUBLIC OF CHINA
Z. Li, S.W. Inst Physics, PEOPLE'S REPUBLIC OF CHINA
Prof. J.A.C. Cabral, Instituto Superior Tecnico, PORTUGAL
Dr. O. Petrus, AL I CUZA Univ., ROMANIA
Dr. J. de Villiers, Fusion Studies, AEC, S. AFRICA
Prof. M.A. Hellberg, Univ. of Natal, S. AFRICA
Prof. D.E. Kim, Pohang Inst. of Sci. & Tech., SO. KOREA
Prof. C.I.E.M.A.T, Fusion Division Library, SPAIN
Dr. L. Stenflo, Univ. of UMEA, SWEDEN
Library, Royal Inst. of Technology, SWEDEN
Prof. H. Wilhelmson, Chalmers Univ. of Tech., SWEDEN
Centre Phys. Des Plasmas, Ecole Polytech, SWITZERLAND
Bibliotheek, Inst. Voor Plasma-Fysica, THE NETHERLANDS
Asst. Prof. Dr. S. Cakir, Middle East Tech. Univ., TURKEY
Dr. V.A. Glukhikh,Sci. Res. Inst. Electrophys.I Apparatus, USSR
Dr. D.D. Ryutov, Siberian Branch of Academy of Sci., USSR
Dr. G.A. Eliseev, I.V. Kurchatov Inst., USSR
Librarian, The Ukr.SSR Academy of Sciences, USSR
Dr. L.M. Kovrizhnykh, Inst. of General Physics, USSR
Kernforschungsanlage GmbH, Zentralbibliothek, W. GERMANY
Bibliothek, Inst. Für Plasmaforschung, W. GERMANY
Prof. K. Schindler, Ruhr-Universität Bochum, W. GERMANY
Dr. F. Wagner, (ASDEX), Max-Planck-Institut, W. GERMANY
Librarian, Max-Planck-Institut, W. GERMANY
Prof. R.K. Janev, Inst. of Physics, YUGOSLAVIA

DATE
FILMED
12/27/93

END